

Narrow spectral linewidth of single zinc-blende GaN/AlN self-assembled quantum dots

S. Sergent,^{1,a)} S. Kako,² M. Bürger,³ D. J. As,³ and Y. Arakawa^{1,2}

¹*Institute for Nano Quantum Information Electronics, The University of Tokyo, 4-6-1 Komaba, Meguro, Tokyo 153-8505, Japan*

²*Institute of Industrial Science, The University of Tokyo, 4-6-1 Komaba, Meguro, Tokyo 153-8505, Japan*

³*Department Physik, Universität Paderborn, Warburger Str. 100, 33098 Paderborn, Germany*

(Received 5 August 2013; accepted 24 September 2013; published online 10 October 2013)

We study by microphotoluminescence the optical properties of single self-assembled zinc-blende GaN/AlN quantum dots grown by plasma-assisted molecular beam epitaxy. As opposed to previous reports, the high quality of such zinc-blende GaN quantum dots allows us to evidence a weak acoustic phonon sideband as well as a limited spectral diffusion. As a result, we report on resolution-limited quantum dot linewidths as narrow as $500 \pm 50 \mu\text{eV}$. We finally confirm the fast radiative lifetime and high-temperature operation of such quantum dots. © 2013 AIP Publishing LLC. [<http://dx.doi.org/10.1063/1.4824650>]

Because of their large exciton binding energy and their large band offsets, GaN quantum dots (QDs) are promising solid state emitters for devices operating at high temperature such as nanolasers, single photon sources, and quantum information devices. Although less mature than their group-III arsenide counterparts, a good understanding of self-assembled polar wurtzite-phase (WZ) GaN QDs has been reached with evidences of their exciton fine structure¹ as well as thorough studies of their polarization properties² and their biexciton behavior.^{3–5} Moreover, polar GaN QDs have already been proven to behave as single photon emitters up to 200 K.⁶ However, the potential of such self-assembled polar QDs is hindered by the presence of a giant built-in electric field that extends their radiative lifetime^{7,8} and broadens their spectral linewidth via an enhanced spectral diffusion.⁹ Besides, the presence of an intense acoustic phonon sideband¹⁰ suggests that the destruction of phase coherence by phonon scattering would limit their use in quantum information applications. Because of the absence of spontaneous polarization in the zinc-blende (ZB) phase of group-III nitrides, ZB GaN QDs are a good alternative to their WZ counterpart and should exhibit reduced spectral diffusion and much shorter radiative lifetimes.¹¹ However, the ZB phase of group-III nitrides is metastable and high quality epilayers free of WZ-phase inclusions prove difficult to grow.¹² As a result, the spectroscopy of single ZB GaN QDs have been so far very limited with a single report on the cathodoluminescence of QDs that showed a significant broadening and an intense acoustic phonon sideband.¹³ Recently, atomically flat ZB AlN free of WZ inclusions has been achieved by plasma-assisted molecular beam epitaxy¹⁴ and has allowed the growth of high-quality ZB GaN QDs.¹⁵ In this work, we study by microphotoluminescence (μPL) the optical properties of single ZB GaN QDs grown by this technique. We especially evidence their fast radiative recombination, a high-temperature operation, a weak acoustic phonon sideband, and a very limited spectral diffusion leading to a resolution-limited linewidth as narrow as $500 \pm 50 \mu\text{eV}$.

Self-assembled Stranski-Krastanov ZB GaN QDs embedded in a 70-nm-thick ZB AlN are grown by plasma-assisted molecular beam epitaxy on a 3C-SiC/Si(100) substrate.¹⁵ Because of the high density of QDs obtained by this growth process ($>10^{11} \text{ cm}^{-2}$), sub-micrometer mesas with nominal diameters ranging from 200 to 500 nm are then processed in the epilayer to reduce the amount of QDs probed by the μPL setup. The QD sample is placed in a He-cooled cryostat and excited in grazing incidence geometry by a frequency-quadrupled continuous-wave (CW) laser or the third harmonic of an 80 MHz Ti-Sapphire pulsed laser, both emitting at 266 nm. The μPL signal is collected by a microscope objective (numerical aperture 0.4), dispersed on a 2400 grooves/mm grating and collected by a nitrogen-cooled charge-coupled device camera. The overall spectral resolution of the setup is 0.5 meV at 4 eV. Unless specified otherwise, the integration time of spectra is 10 s. The time-resolved experiments are conducted by time correlated single photon counting: the signal is spectrally filtered by a slit after dispersion on the grating, and it is then collected by a photomultiplier detector (200 ps time-resolution); the latter is connected to a time interval counter that measures the delay between a trigger generated by the pulsed laser and a photon hitting the photomultiplier.

The μPL spectrum of the QD ensemble measured on unpatterned areas of the sample presents a Gaussian distribution centered at 3.49 eV with a 187 meV full-width at half-maximum (FWHM), as depicted in Fig. 1(a). Time-resolved measurements taken over the PL ensemble spectral range exhibit single-exponential decays suggesting that the radiative lifetime of the QD ensemble is shorter than $\tau_r = 390 \text{ ps}$ (Fig. 1(b)). This is close to the setup resolution and in fair agreement with previous reports.¹¹ When probing unpatterned areas or sub-micrometer mesas with the CW laser, single lines can be found on the higher energy side of the QD ensemble PL between 3.5 eV and 4.3 eV (Fig. 1(a)). The integrated intensity of most lines exhibits a linear dependence to the laser excitation power that suggests that they originate from exciton recombinations in individual ZB GaN QDs. The radiative lifetimes of such excitons as measured by

^{a)}Author to whom correspondence should be addressed. Electronic mail: ssergent@iis.u-tokyo.ac.jp

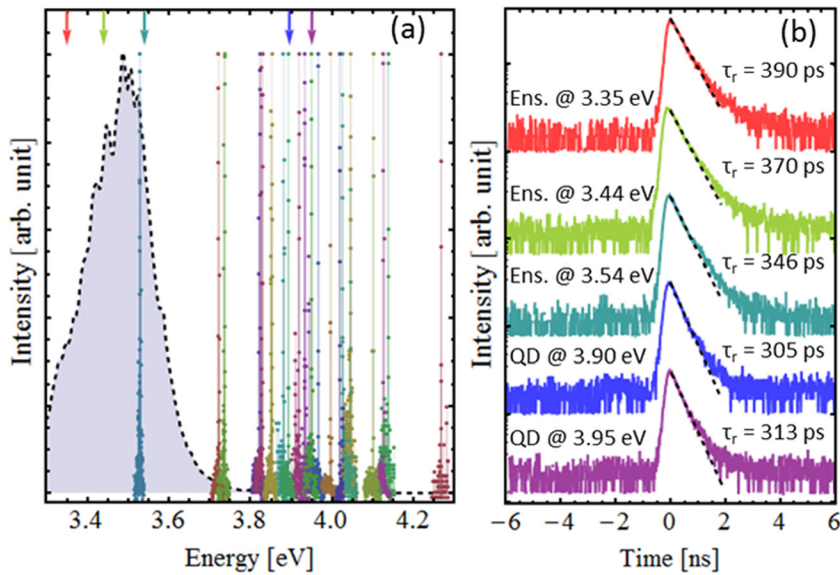


FIG. 1. (a) Normalized μ PL spectra of single ZB GaN QD lines measured at $T = 4$ K for various mesas. The dashed line corresponds to the QD ensemble μ PL on a non-patterned area of the sample. (b) Time-resolved PL decay curves of the QD ensemble at 3.35 eV, 3.44 eV, 3.54 eV and of single QDs emitting at 3.90 eV and 3.95 eV. For each curve, the detection wavelength is highlighted by a colored arrow in (a). The decay times are, respectively, 390 ± 2 ps, 374 ± 2 ps, 346 ± 2 ps, 305 ± 2 ps, and 313 ± 3 ps (no deconvolution; resolution limit: 200 ps).

time-resolved μ PL at higher energies are only slightly shorter than the decays measured on the QD ensemble (Fig. 1(b)), confirming the absence of a giant built-in electric field in such single non-polar ZB QDs.

In semiconductor QDs, the so-called spectral diffusion arises from the trapping and release of free carriers by defects in the QD vicinity. The subsequent change in the electrostatic environment of the QD leads to time-dependent spectral shifts that are especially large in self-assembled WZ GaN QDs because of their giant built-in electric field.⁹ If the change of the electrostatic environment of the QD takes place on a time scale shorter than the integration time, then the jitter broadens the measured emission linewidth that is not defined by the QD coherence time any more. If the change takes place on a time scale longer than the integration time, then it is possible to observe the spectral shift of the QD emission. As a result of the non-polar aspect of ZB GaN QDs, the spectral diffusion on both scales should be much smaller than in the WZ phase. This is what we observe on the short-time scale, as a large number of QDs present linewidths narrower than 1 meV (Fig. 2(a)), and a 500 ± 50 μ eV resolution-limited linewidth can even be measured (Fig. 2(b)). This is similar to the narrowest linewidths observed in non-polar WZ GaN QDs.¹⁶ However, single QD lines exhibiting broadening as large as 6.5 meV have also been measured (Fig. 2(a)). As well-known in other semiconductor systems,¹⁷ this is likely due to the close proximity of surface states created by the mesa processing that act as free carrier traps and strongly broadens the QD emission. Comparing the average linewidth $\gamma^{200\text{nm}} = 1.8 \pm 0.8$ meV of QDs embedded in the smallest mesas to the average linewidth $\gamma^\infty = 810 \pm 340$ μ eV of QDs found in unpatterned regions of the sample supports this claim. It is worth mentioning that the linewidth of QDs characterized in this work exhibit a downward trend for increasing energies, i.e., decreasing size (Fig. 2(a)). This size-dependent spectral diffusion suggests that there exists a residual exciton permanent dipole in ZB GaN QDs, despite the fact that the piezoelectric potential is smaller than the WZ GaN QD's by an order of magnitude.¹⁸ On the long-time scale, the evolution of single ZB GaN QDs also reveals significant spectral fluctuations. The μ PL spectra of

Fig. 2(c) present the time evolution of two QD emission lines. The lines exhibit synchronized fluctuations of the central energy as highlighted by the black dots in Fig. 2(c). The average emission energies of each line are $E_1 = 3.9889$ eV and $E_2 = 3.9875$ eV and the standard deviation of the central energies is $\sigma = 0.6$ meV, which is a representative value of the long-time scale spectral diffusion. QDs found in other mesas exhibit a standard deviation σ of the exciton peak central energy that ranges between $\sigma_{\text{min}} = 0.12$ meV and $\sigma_{\text{max}} = 0.8$ meV with no clear dependence on emission energy or excitation power. This is of the same order of magnitude as spectral shifts observed in other non-polar GaN QDs.¹⁹ Moreover, as opposed to WZ self-assembled GaN QDs studied at the same excitation power,⁹ the ZB GaN QDs do not exhibit any discrete spectral jump in the meV range. This supports the idea of a rather small built-in electric field.

As can be seen from the error bars in Fig. 2(a), for most μ PL spectra measured at low temperature, the QD zero phonon line is symmetric and can be accurately fitted by a Gaussian curve (Fig. 2(b)). On the contrary to single ZB GaN QDs¹³ and WZ GaN QDs¹⁰ previously observed by cathodoluminescence, a low energy sideband that could be attributed to the inelastic scattering of acoustic phonons with charge carriers is rarely observed. On the one hand, the low piezoelectric potential calculated in ZB GaN QDs¹⁸ should have a significantly weaker contribution to the acoustic phonon sideband than for WZ GaN QDs.¹⁰ On the other hand, a weak acoustic phonon sideband is anyway what one expects in ZB GaN QDs because the reduced spectral diffusion increases the relative peak intensity of the zero phonon line. Of course the latter argument does not hold for ZB QDs presenting a significant broadening at low temperature. As a result, QDs presenting a large error bar on the Gaussian fitting and a large broadening correspond to asymmetric line shapes presenting a sideband attributed to the coupling of excitons to acoustic phonons (see inset of Fig. 2(a)). It incidentally shows that at energies lower than the exciton state, there is a quasi-continuum of radiative states that constitute the final states of the acoustic phonons relaxation.

As the temperature increases, the zero-phonon line remains symmetric and for some QDs it broadens linearly,

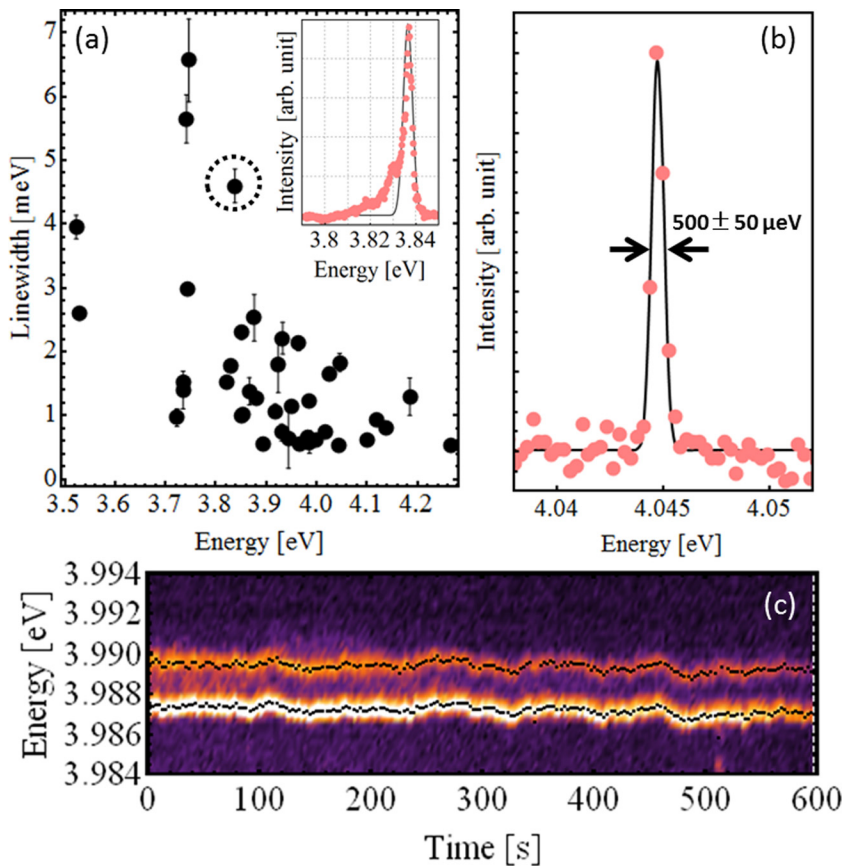


FIG. 2. (a) Linewidth of all the observed single QDs at $T=4\text{K}$ under CW excitation as calculated from a Gaussian fitting. The Gaussian behavior expresses either the statistical change in the QD environment leading to the spectral diffusion or the broadening due to the optical setup resolution. The bars correspond to the fitting error. The dashed circle highlights a specific data point whose spectrum is shown in the inset. The black line is a Gaussian fitting to the data. For all measurements, the spectral resolution is 0.5meV at 4eV . (b) μPL spectrum of a single QD observed on an unpatterned area of the sample at $T=4\text{K}$ and under a $4\text{kW}\cdot\text{cm}^{-2}$ CW excitation power. The black line is a Gaussian fitting to the data. (c) Time-dependent spectrum of a single QD observed in a 500nm mesa at $T=4\text{K}$ and under a $4\text{kW}\cdot\text{cm}^{-2}$ CW excitation power. A spectrum is taken every 3s . The black dots highlight the central energy of each QD line as deduced from a Gaussian fitting.

up to $T=75\text{K}$ (Figs. 3(a) and 3(b)). Beyond 75K , the linewidth increases exponentially and a low-energy sideband appears, superimposed to the zero-phonon line and breaking the lineshape symmetry. The latter behavior has been observed in other semiconductor systems²⁰ and is usually understood as the recombination of excitons assisted by the emission or absorption of acoustic phonons. Although the broadening of the QD line shape is often described by an extension of the Huang-Rhys theory in the frame of the independent Boson model,^{10,21} the model fails to explain the broadening of the zero-phonon line sometimes observed at low temperature. Various effects have been proposed to explain this behavior such as coupling of exciton to phonon damped by scattering at pattern surfaces²² or motional narrowing.²³ Although the high excitation power used here makes motional narrowing unlikely, it is far beyond the scope of this paper to discriminate between those phenomena. In order to phenomenologically account for the behaviors observed in the low and high temperature ranges, we can fit the temperature broadening of the zero-phonon line as follows: $\gamma = \gamma_0 + \alpha \times T + b \times [e^{-\frac{E_a}{k_B T}} - 1]^{-1}$, with γ_0 the zero-phonon linewidth at $T=0\text{K}$, E_a the energy describing an activated coupling to phonon that is predominant in the high temperature range, and α the broadening efficiency of the zero-phonon line in the low temperature range. For two QDs found in two different mesas and emitting, respectively, at 3.97eV and 3.99eV (see gray and black circles in Fig. 3(b)) we find $\gamma_0 = 0.58 \pm 0.03\text{meV}$ (resp. $0.84 \pm 0.09\text{meV}$), $E_a = 48 \pm 8\text{meV}$ (resp. $32 \pm 4\text{meV}$), and $\alpha = 3.2 \pm 0.8\ \mu\text{eV}\cdot\text{K}^{-1}$ (resp. within the error range). Let us mention that the broadening efficiency α found here is of the

same order of magnitude as values reported in the literature for other QD systems.^{20,22–24} However, the spectral diffusion and the spectral setup resolution tend to hide the homogeneous broadening of the zero-phonon line, so that the measured value of α actually constitutes a lower limit. Finally, despite the significant broadening of excitonic lines, the emission of single QDs can be observed at temperatures as high as 205K (Fig. 3(a)), owing to the large band offsets between ZB GaN and ZB AlN and to the large binding energy of excitons in GaN QDs.

As a conclusion, we have evidenced the high optical quality of single ZB GaN QDs grown by plasma-assisted molecular beam epitaxy. The absence of spontaneous polarization limits the spectral diffusion in our ZB GaN QDs, leading to a resolution-limited linewidth as narrow as $500 \pm 50\ \mu\text{eV}$, which compares favorably with previously reported ZB GaN QDs.¹³ As expected, we showed that the absence of giant built-in electric field also leads to radiative lifetimes of individual QDs that are much shorter than for WZ GaN QDs. This is of prime importance for the use of ZB GaN QDs in high-speed operation devices and applications that require large oscillator strength. The absence of acoustic phonon sideband below 75K found in some QDs is another advantage over self-assembled WZ GaN QDs.¹⁰ It should limit the dephasing of quantum processes by phonon scattering and might allow for quantum applications operating at higher temperatures than in other semiconductor systems.²⁵ Excitonic recombinations in single ZB GaN QDs can be followed up to 205K , thus showing good prospects for the use of ZB GaN QDs in optical devices operating at high temperature such as single photon sources. Overall the demonstration of ZB GaN QDs

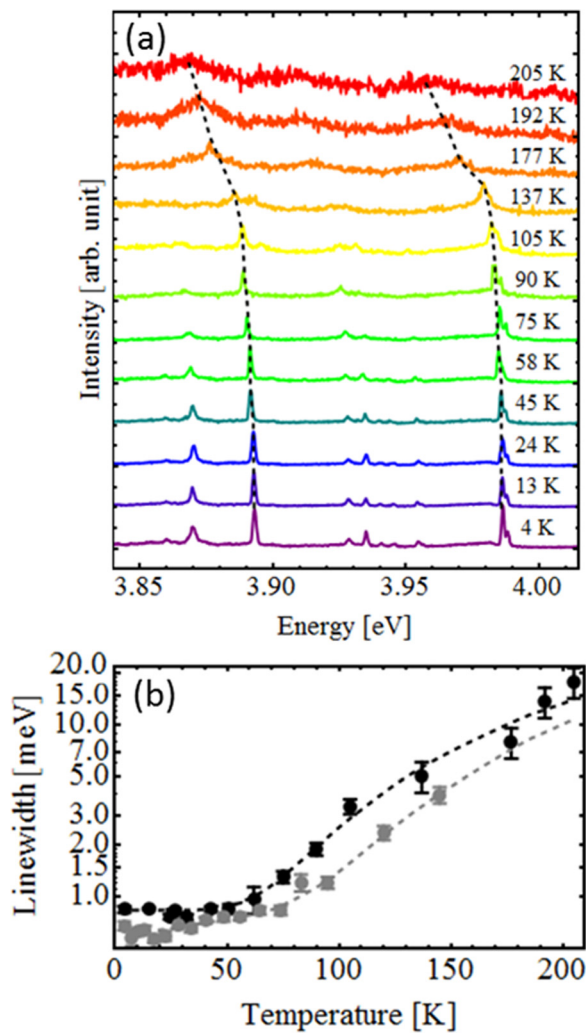


FIG. 3. (a) Normalized temperature-dependent μ PL spectra of various QDs embedded in a 500 nm mesa under an $8 \text{ kW} \cdot \text{cm}^{-2}$ CW excitation power. The dashed lines are guides for the eyes. (b) Linewidths of QD emission peaks originating from two different 500-nm mesas as a function of temperature. The black circles correspond to the QD emitting at 3.99 eV in (a). The gray circles correspond to a QD emitting at 3.97 eV. The dashed lines are a fitting curve of the form $\gamma = \gamma_0 + \alpha \times T + b \times [e^{-\frac{E_g}{k_B T}} - 1]^{-1}$. The vertical bars are error on the Gaussian fitting of QD peaks.

presenting a high optical quality will allow for the study of a larger set of their fundamental properties (polarization properties, fine structure, behavior of excitonic, and multiexcitonic complexes), and it opens the path to the fabrication of a wide spectrum of devices with better prospects than for self-assembled WZ GaN QDs.

This work was supported by the Project for Developing Innovation Systems of the Ministry of Education, Culture, Sports, Science, and Technology (MEXT), by Japan Society

for the Promotion of Science (JSPS) through its “Funding Program for world-leading Innovation R&D on Science and Technology” (FIRST Program), and by the DFG graduate program GRK 1464 “Micro- and Nanostructures in Optoelectronics and Photonics.”

- ¹C. Kindel, S. Kako, T. Kawano, H. Oishi, Y. Arakawa, G. Hönig, M. Winkelkemper, A. Schliwa, A. Hoffmann, and D. Bimberg, *Phys. Rev. B* **81**, 241309(R) (2010).
- ²R. Bardoux, T. Guillet, B. Gil, P. Lefebvre, T. Bretagnon, T. Talierno, S. Rousset, and F. Semond, *Phys. Rev. B* **77**, 235315 (2008).
- ³S. Kako, K. Hoshino, S. Iwamoto, S. Ishida, and Y. Arakawa, *Appl. Phys. Lett.* **85**, 64 (2004).
- ⁴D. Simeonov, A. Dussaigne, R. Butté, and N. Grandjean, *Phys. Rev. B* **77**, 075306 (2008).
- ⁵C. Kindel, S. Kako, T. Kawano, H. Oishi, and Y. Arakawa, *Jpn. J. Appl. Phys.* **48**, 04C116 (2009).
- ⁶S. Kako, C. Santori, K. Hoshino, S. Gotzinger, Y. Yamamoto, and Y. Arakawa, *Nature Mater.* **5**, 887 (2006).
- ⁷S. Kako, M. Miyamura, K. Tachibana, K. Hoshino, and Y. Arakawa, *Appl. Phys. Lett.* **83**, 984 (2003).
- ⁸T. Bretagnon, P. Lefebvre, P. Valvin, R. Bardoux, T. Guillet, T. Talierno, B. Gil, N. Grandjean, F. Semond, B. Damilano, A. Dussaigne, and J. Massies, *Phys. Rev. B* **73**, 113304 (2006).
- ⁹R. Bardoux, T. Guillet, P. Lefebvre, T. Talierno, T. Bretagnon, S. Rousset, B. Gil, and F. Semond, *Phys. Rev. B* **74**, 195319 (2006).
- ¹⁰I. A. Ostapenko, G. Honig, S. Rodt, A. Schliwa, A. Hoffmann, D. Bimberg, M.-R. Dachner, M. Richter, A. Knorr, S. Kako, and Y. Arakawa, *Phys. Rev. B* **85**, 081303(R) (2012).
- ¹¹J. Simon, N. Pelekanos, C. Adelman, E. Martinez-Guerrero, R. André, B. Daudin, L. S. Dang, and H. Mariette, *Phys. Rev. B* **68**, 035312 (2003).
- ¹²V. Lebedev, V. Cimalla, U. Kaiser, Ch. Foerster, J. Pezoldt, J. Biskupek, and O. Ambacher, *J. Appl. Phys.* **97**, 114306 (2005).
- ¹³J. P. Garayt, J.-M. Gérard, F. Enjalbert, L. Ferlazzo, S. Founta, E. Martinez-Guerrero, F. Rol, D. Araujo, R. Cox, B. Daudin, B. Gayral, L. S. Dang, and H. Mariette, *Physica E* **26**, 203 (2005).
- ¹⁴T. Schupp, K. Lischka, and D. J. As, *J. Cryst. Growth* **312**, 1500 (2010).
- ¹⁵T. Schupp, T. Meisch, B. Neuschl, M. Feneberg, K. Thonke, K. Lischka, and D. J. As, *Phys. Status Solidi C* **8**, 1495 (2011).
- ¹⁶F. Rol, B. Gayral, S. Founta, B. Daudin, J. Eymery, J.-M. Gérard, H. Mariette, Le Si Dang, and D. Peyrade, *Phys. Status Solidi B* **243**, 1652 (2006).
- ¹⁷C. F. Wang, A. Badolato, I. Wilson-Rae, P. M. Petroff, E. Hu, J. Urayama, and A. Imamoğlu, *Appl. Phys. Lett.* **85**, 3423 (2004).
- ¹⁸V. A. Fonoberov and A. A. Balandin, *J. Appl. Phys.* **94**, 7178 (2003).
- ¹⁹F. Rol, S. Founta, H. Mariette, B. Daudin, Le Si Dang, J. Bleuse, D. Peyrade, J.-M. Gerard, and B. Gayral, *Phys. Rev. B* **75**, 125306 (2007).
- ²⁰L. Besombes, K. Kheng, L. Marsal, and H. Mariette, *Phys. Rev. B* **63**, 155307 (2001).
- ²¹B. Krummheuer, V. M. Axt, and T. Kuhn, *Phys. Rev. B* **65**, 195313 (2002).
- ²²G. Ortner, D. R. Yakovlev, M. Bayer, S. Rudin, T. L. Reinecke, S. Fafard, Z. Wasilewski, and A. Forchel, *Phys. Rev. B* **70**, 201301(R) (2004).
- ²³I. Favero, A. Berthelot, G. Cassabois, C. Voisin, C. Delalande, Ph. Roussignol, R. Ferreira, and J. M. Gérard, *Phys. Rev. B* **75**, 073308 (2007).
- ²⁴S. Amloy, K. H. Yu, K. F. Karlsson, R. Farivar, T. G. Andersson, and P. O. Holtz, *Appl. Phys. Lett.* **99**, 251903 (2011).
- ²⁵A. J. Ramsay, T. M. Godden, S. J. Boyle, E. M. Gauger, A. Nazir, B. W. Lovett, A. M. Fox, and M. S. Skolnick, *Phys. Rev. Lett.* **105**, 177402 (2010).